The generalized Hubbard model applied to triplet p-wave pairing in $Sr_{1-x}K_xFe_2As_2$

M. Martínez

Facultad de Ciencias Físico Matemáticas, Benemérita Universidad Autónoma de Puebla, Ciudad Universitaria, 4 Sur 104 Centro Histórico 72000, Cd. de Puebla, México.
e-mail: marijosse.martinez@alumno.buap.mx

J. S. Millán and O. Pavón-Torres

Universidad Politécnica de la Energía, Carretera Cruz Azul Bomintza Km 3.1, 42820, Tula de Allende, Hidalgo, México.
e-mail: jsmmalo@gmail.com; omar.pavon@upenergia.edu.mx

L. A. Pérez,

Instituto de Física, Universidad Nacional Autónoma de México, 04510, Ciudad de México, México.
e-mail: lperez@fisica.unam.mx

Received 3 June 2025; accepted 11 September 2025

Currently, several superconductors with singlet pairing of d-wave symmetry are known, but very few triplet-pairing superconductors have been found. It is believed that Sr_2RuO_4 and some uranium compounds such as UTe_2, with very low critical temperatures (T_c) around 1 K, could have Cooper pairs in a triplet state. Other possible candidates that could present triplet pairing are magnetic compounds based on Fe, for example $Sr_{1-x}K_xFe_2As_2$, which have optimal doping around $x = 0.5$ with maximum critical temperature $T_{c-\max} = 37$ K. On the other hand, p-wave pairing in a slightly distorted square lattice, described by a generalized Hubbard model, has been investigated considering that the next-nearest neighbor correlated hopping interactions along the two lattice diagonals are slightly different. In this work, we investigate the appearance of triplet-pairing p-wave superconducting states in square lattices where the electron dynamics is described by the generalized Hubbard model. An optimal electron density (n_{op}), where the maximum critical temperature occurs, was found for each value of the ratio between the next-nearest neighbor and the nearest-neighbor one-electron hoppings ($-t^{'}/t$), and a search of Hamiltonian parameters was performed to fit T_c as a function of x in the compound $Sr_{1-x}K_xFe_2As_2$. In particular, the set of Hamiltonian parameters providing the best fit is $\Delta t = 0.5$ eV, $\Delta t_3 = 0.05$ eV and $\delta_3 = 0.08$ eV, with the ratio $-t^{'}/t = 0.29$ adjusted to obtain a maximum of the critical temperature of $T_{c-\max} \approx 36$ K at $n_{op} = 0.50$, which agrees with the maximum critical temperature (≈ 37 K) of the compound $Sr_{0.5}K_{0.5}Fe_2As_2$. With this set of Hamiltonian parameters, other superconducting properties were calculated, such as the amplitude of the p-wave superconducting gap, the ground-state and condensation energies, and the electronic specific heat as a function of the temperature and its jump at T_c. Additionally, a comparison between the ground states energies of the d- and p-wave superconducting states was made, finding that the p-wave superconducting state has the lowest energy and it can be considered as the ground state. Hence, the compound $Sr_{1-x}K_xFe_2As_2$ can be studied under the assumption of triplet pairing with a p-wave superconducting gap symmetry, and probably other similar pnictides, such as $Ba_{0.4}K_{0.6}Fe_2As_2$ with $T_c = 38$ K, may also exhibit p-wave triplet pairing.

Keywords: Theories and models of superconducting state; pairing symmetries (other than s-wave); $Sr_{1-x}K_xFe_2As_2$

DOI: https://doi.org/10.31349/RevMexFis.72.021601

1. Introduction

Superconductivity in iron-based pnictides has attracted extensive attention since its discovery [1], not only because of the relatively high critical temperatures (T_c) [2], but also due to the variety of pairing symmetries proposed for these materials [3, 4]. While most known superconductors exhibit singlet pairing with s- or d-wave gap symmetry, possible cases of triplet superconductivity include Sr_2RuO_4 and uranium-based compounds such as UTe_2, both with very low T_c values close to 1 K [5, 6]. Identifying triplet superconductors with higher T_c is therefore of fundamental importance, as triplet states are expected to be robust under magnetic fields [6], making them suitable for applications in superconducting magnets, spintronics, and potentially quantum computing. The compound $Sr_{1-x}K_xFe_2As_2$ (with $T_{c-\max} \approx 37$ K at $x = 0.5$) provides an interesting case [3, 7], since experimental evidence has not yet resolved whether its superconducting gap symmetry corresponds to s-, d-, or even p-wave. This uncertainty opens the possibility that pnictides could present triplet states at relatively high critical temperatures. In this context, theoretical approaches capable of treating different superconducting symmetries within the same formalism are essential. The generalized Hubbard model, which extends the conventional Hubbard Hamiltonian by including correlated hopping (or bond-charge) interactions, provides such

a framework. It has been successfully applied to describe singlet states of s- and d-wave symmetry and can also be extended to explore the emergence of triplet p-wave pairing [8–10]. In this work, we use the generalized Hubbard model to investigate the stability of p-wave superconducting states in $Sr_{1-x}K_xFe_2As_2$. By carefully selecting Hamiltonian parameters, the experimental maximum critical temperature can be theoretically reproduced. Also, other superconducting properties, such as the gap amplitude, condensation energy, and electronic specific heat can be obtained. Our analysis highlights the conditions under which p-wave symmetry becomes energetically favorable, suggesting that triplet pairing may indeed play a role in these compounds. Given that the amplitude of the superconducting gap is two orders of magnitude lower for p-wave than d-wave symmetry, the discernment of the ground state is important; this distinction can help to improve the performance of technological applications, for example in superconducting cables. The critical current density (J_c) is expected to be proportional to the gap amplitude [11, 12], therefore, for a superconductor $J_{c-pw} < J_{c-dw}$. Another important consideration to take into account is the Cooper pairs formations, while for the p-wave symmetry the spatial part is antisymmetric, for the d-wave is symmetric, and their spins are parallel or antiparallel, respectively [13]. Hence, the influence of the magnetic field in a superconductor with p-wave symmetry should be different from that of d-wave. The superconductor with p-wave symmetry can support a higher magnetic field without loss of its superconducting properties.

2. The model

We start from the single-band Generalized Hubbard Hamiltonian ($\hat{H}$) with on-site Coulombic interaction (U), first-(Δt) and second-neighbour (Δt_3) correlated-hopping interactions [14]:

$$\hat{H} = H_1 + H_{\text{int}}, \tag{1}$$

where

$$H_1 = t \sum_{\langle i,j\rangle,\sigma} c^\dagger_{i,\sigma} c_{j,\sigma} + t' \sum_{\langle\langle i,j\rangle\rangle,\sigma} c^\dagger_{i\sigma} c_{j\sigma}, \tag{2}$$

$$H_{\text{int}} = U \sum_i n_{i\uparrow} n_{i\downarrow} + \Delta t \sum_{\langle i,j\rangle,\sigma} c^\dagger_{i,\sigma} c_{j,\sigma} (n_{i,-\sigma} + n_{j,-\sigma}) + \Delta t_3 \sum_{\langle i,l\rangle\langle j,l\rangle\langle\langle i,j\rangle\rangle,\sigma} c^\dagger_{i,\sigma} c_{j,\sigma} n_l. \tag{3}$$

Here, $n_i = n_{i,\uparrow} + n_{i,\downarrow}, n_{i,\sigma} = c^\dagger_{i,\sigma} c_{i,\sigma}$, and $c^\dagger_{i,\sigma}(c_{i,\sigma})$, is the creation (annihilation) operator with spin $\sigma = \downarrow$ or $\uparrow$ at site i. $\langle i,j\rangle$ and $\langle\langle i,j\rangle\rangle$ denote nearest- and next-nearest neighbor sites. The expressions for the parameters in this model are given in Ref. [14]. To address p-wave pairing, an infinitesimal distortion of the square lattice is considered. This distortion can break the degeneracy of the p-wave pairing states in a non-distorted square lattice, and then the energy of these p-wave states can be separated and one of them can shift below the energies of s- or d-wave superconducting states and becoming the ground state [10]. Therefore, we consider slightly different next-nearest-neighbor hoppings (t') and correlated hopping interactions (Δt_3) along the two diagonal directions $\hat{x} \pm \hat{y}$ of a square lattice. Hence, their new values are $t'_\pm = t' \pm \delta$ and $\Delta t_3^\pm = \Delta t_3 \pm \delta_3$, where $\pm$ refers to the $\hat{x} \pm \hat{y}$ direction.

The operators of Eq. (1) can be transformed into the reciprocal space by a Fourier transformation $c^\dagger_{\mathbf{k},\sigma} = (1/N_s)\sum_j \exp(i\mathbf{k}\cdot\mathbf{R}_j) c^\dagger_{j,\sigma}$, and the Hamiltonian becomes:

$$\hat{H} = \sum_{k,\sigma} \varepsilon(\mathbf{k}) c^\dagger_{k,\sigma} c_{k,\sigma} + \frac{1}{N_s} \sum_{\mathbf{k},\mathbf{k}',\mathbf{q},\sigma} W_{\mathbf{k},\mathbf{k}',\mathbf{q}} c^\dagger_{\mathbf{k}+\mathbf{q},\sigma} c^\dagger_{-\mathbf{k}+\mathbf{q},\sigma} c_{-\mathbf{k}'+\mathbf{q},\sigma} c_{\mathbf{k}'+\mathbf{q},\sigma}, \tag{4}$$

where N_s is the total number of lattice sites, $\varepsilon(\mathbf{k})$ is the dispersion relation of single electrons in the square lattice and $W_{\mathbf{k},\mathbf{k}',\mathbf{q}}$ is the interaction potential for electrons with the same spin projection and it is given by:

$$W_{\mathbf{k},\mathbf{k}',\mathbf{q}} = \Delta t_3^+ \gamma(\mathbf{k}+\mathbf{q}, \mathbf{k}'+\mathbf{q}) + \Delta t_3^- \zeta(\mathbf{k}+\mathbf{q}, -\mathbf{k}'+\mathbf{q}), \tag{5}$$

with

$$\beta(\mathbf{k}) = 2[\cos(k_x a) + \cos(k_y a)], \tag{6}$$

$$\gamma(\mathbf{k}.\mathbf{k}') = 2\cos[a(k_x + k'_y)] + 2\cos[a(k'_x + k_y)], \tag{7}$$

$$\zeta(\mathbf{k}.\mathbf{k}') = 2\cos[a(k_x - k'_y)] + 2\cos[a(k'_x - k_y)], \tag{8}$$

where a is the lattice parameter. Notice that the interaction potential $W_{\mathbf{k},\mathbf{k}',\mathbf{q}}$ does not depend on Δt, since this term only contributes when the electron spin projections are different.

If we assume a p-wave superconducting gap of the form:

$$\Delta(\mathbf{k}) = \Delta_p[\sin(k_x a) \pm \sin(k_y a)], \tag{9}$$

where Δ_p is the p-wave gap amplitude, the chemical potential (μ) and superconducting gap amplitude $[\Delta_p]$ can be obtained from the mean-field BCS coupled equations [14]:

$$1 = \pm \frac{4\delta_3 a^2}{4\pi^2} \int\int_{1BZ} \times \left\{ \frac{[\sin(k_x a) \pm \sin(k_y a)]^2}{2E(\mathbf{k})} \times \tanh\left(\frac{E(\mathbf{k})}{2k_B T}\right) \right\} dk_x dk_y, \tag{10}$$

$$n - 1 = -\frac{a^2}{4\pi^2} \int\int_{1BZ} \frac{\varepsilon(\mathbf{k}) - \mu}{E(\mathbf{k})} \times \tanh\left(\frac{E(\mathbf{k})}{2k_B T}\right) dk_x dk_y, \tag{11}$$

where $1BZ$ is the first Brillouin zone of a square lattice, defined as

$$\left[\frac{-\pi}{a},\frac{\pi}{a}\right]\otimes\left[\frac{-\pi}{a},\frac{\pi}{a}\right].$$

The quasi-particle energy $[E(\mathbf{k})]$ is given by:

$$E(\mathbf{k})=\sqrt{(\varepsilon_{MF}-\mu)^2+\Delta^2(\mathbf{k})}, \tag{12}$$

where the mean-field dispersion relation (ε_{MF}) is:

$$\begin{aligned}\varepsilon_{MF}(\mathbf{k}) &= \varepsilon_0+2t_{MF}[\cos(k_xa)+\cos(k_ya)]\\ &+2t'_{MF,+}\cos[a(k_x+k_y)]\\ &+2t'_{MF,-}\cos[a(k_x-k_y)],\end{aligned} \tag{13}$$

with

$$\varepsilon_0=\frac{U}{2}n, \tag{14}$$

$$t'_{MF,\pm}=t'_{\pm}+2n\Delta t_3^{\pm}, \tag{15}$$

$$t_{MF}=t+n\Delta t, \tag{16}$$

where n is the electron density.

The critical temperature can be determined from Eq. (10) considering that $\Delta_p\,(T_c)=0$. On the other hand, the ground state energy (E_g) per site is given by [14]:

$$\begin{aligned}E_g &= \sum_{\mathbf{k}}\left[\xi_{MF}(\mathbf{k})-\frac{\xi^2_{MF}(\mathbf{k})}{E(\mathbf{k})}\right]\\ &+\sum_{\mathbf{k}}\frac{\Delta^2(\mathbf{k})}{2E(\mathbf{k})}+\mu N.\end{aligned} \tag{17}$$

Taking into account Eq. (9), Eq. (17) can be simplified as follows (14):

$$\begin{aligned}E_g &= \frac{1}{N_s}\sum_{\mathbf{k}}[\varepsilon_{MF}(\mathbf{k})-E(\mathbf{k})]\\ &+\frac{\Delta_p^2}{4\delta_3-V}+(n-1)\mu.\end{aligned} \tag{18}$$

3. Results

Table I shows the critical temperature $T_{c-\max}$ for p-wave superconducting states with different values of δ_3 and $n_{op}\approx 0.5$. Observe that the set of Hamiltonian parameters with $n=0.5$, $-t^{'}/t=0.29$ and $\delta_3=0.08$ eV lead to a $T_c=36$ K which is very close to that of $Sr_{1-x}K_xFe_2As_2$ with $x=0.5$ and $T_{c-\max}=37$ K.

The optimal electron density (n_{op}) and the corresponding ground state energy for each value of the ratio between next- and nearest-neighbor hopping (t'/t) was determined. The results show that a maximum (minimum) does exist from the set of values $T_{c-\max}$ in low (high) densities [14], see

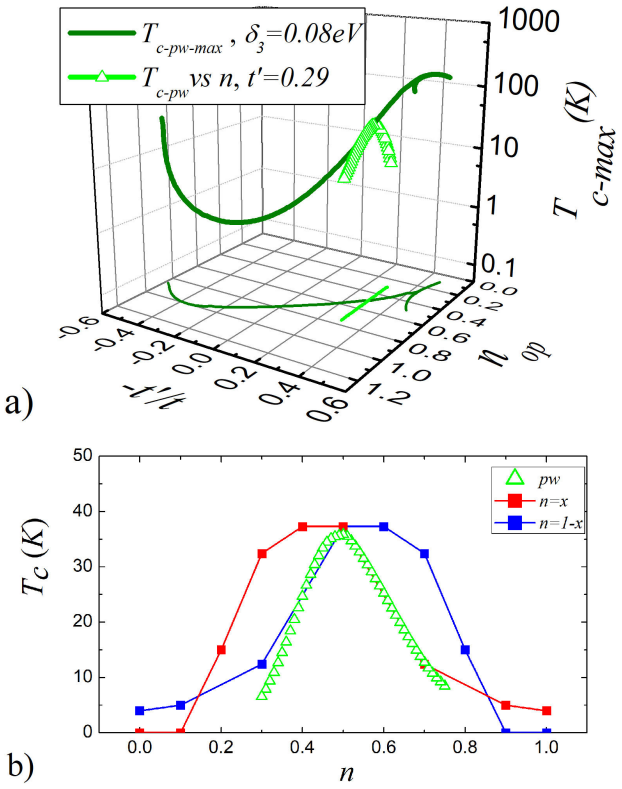

FIGURE 1. a) Maximum critical temperature $T_{c-\max}$ in the space $(-t'/t, n_{op})$ for a system with the Hamiltonian parameters $\Delta t=0.5$ eV, $\Delta t_3=0.05$ eV, $\delta_3=0.08$ eV, $-t'/t=0.29$ (green triangles). b) Calculated critical temperature T_c versus electron doping (n) for a p-wave superconductor in comparison with experimental data for $Sr_{1-x}K_xFe_2As_2$ considering $n=x$ (blue squares) and $n=1-x$ (red squares) [3].

TABLE I. Superconducting critical temperatures (T_c) for different values of δ_3 at n_{op} close to 0.5.

δ_3 (eV)	n_{op}	t'/t	T_c (K)
0.1	0.495	0.300	110
0.09	0.497	0.295	67
0.08	0.500	0.290	36
0.07	0.502	0.275	13
0.06	0.501	0.275	5

Fig. 1a), 1b) shows a comparison between the theoretical p-wave critical temperature (T_c) as a function of the carrier concentration (n) and that experimentally obtained for the compound $Sr_{1-x}K_xFe_2As_2$ [3, 7]. The used Hamiltonian parameters correspond to $\delta_3=0.08$ eV, and $-t'/t=0.29$, and two different cases have been considered for the equivalence between the doping (x) and the carrier density (n), *i.e.*, $n=x$ and $n=1-x$. $n=x$ corresponds to a doping of holes from half filling and the underdoping region matches well with the theoretical results, while if $n=1-x$ the fitting is better for the overdoping region. Figure 2a) shows the p-wave superconducting gap amplitude (Δ_p) and T_c versus the carrier

TABLE II. Superconducting properties for systems with $\Delta t = 0.5$ eV, $\Delta t_3 = 0.05$ eV and $\delta_3 = 0.08$ eV.

n	$t^{'}/t$	T_c(K)	E_g(eV)	Δ_p(eV)	E_{cond}(eV)	E_F(eV)
0.49	0.29	35.6	-0.759994	0.0046208	$6.271\text{x}10^{-6}$	-1.36044
0.50	0.29	35.9	-0.768070	0.0045553	$5.933\text{x}10^{-6}$	-1.35478
0.51	0.29	35.5	-0.776170	0.0043922	$5.513\text{x}10^{-6}$	-1.34674

TABLE III. Critical temperatures and condensation energies for α-symmetry superconducting states. For d-wave superconducting states $\delta = \delta_3 = 0$.

α	n_{op}	$-t^{'}/t$	$T_{c-\max}$	E_{g-T_0}(eV)	E_{g-T_c}(eV)	E_{cond}(eV)
p	0.50	0.29	36	-0.768070	-0.768064	$5.933\text{x}10^{-6}$
d	0.49	0.29	122	-0.73622	-0.736357	0.000134

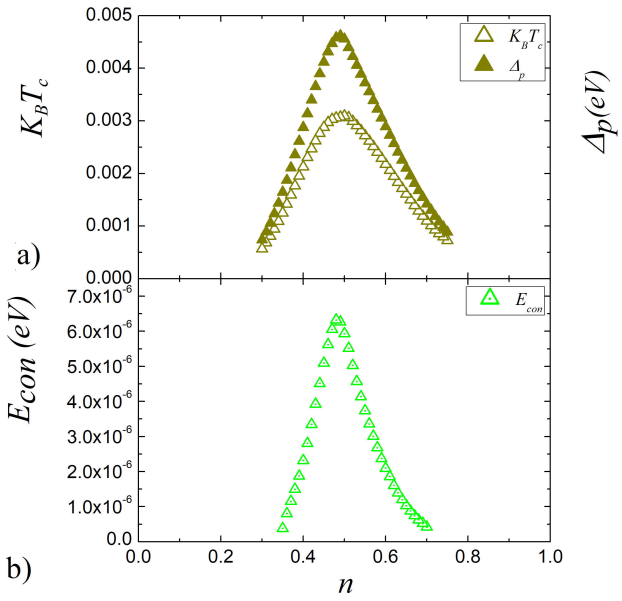

FIGURE 2. a) Superconducting gap amplitude (Δ_p) and T_c and (b) condensation energy (E_{con}) versus electron concentration (n), for a system with the same Hamiltonian parameters as in Fig. 1.

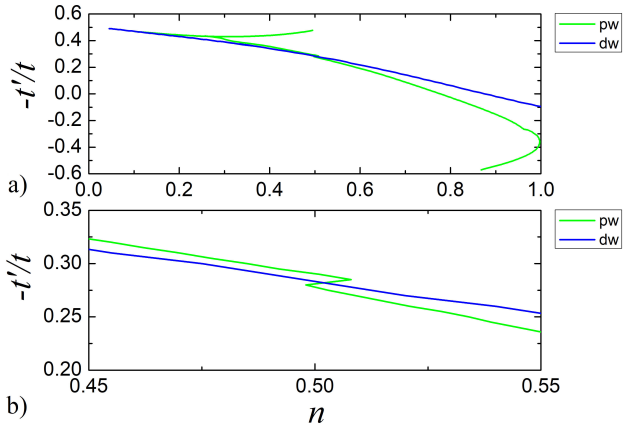

FIGURE 3. a). Phase diagram in the space $(-t'/t, n)$ for the location of the optimal carrier density n_{op} of α-symmetry superconducting states, with $\alpha =$ p- (green) and d-wave (blue lines). b) Amplification around $n_{op} = 0.5$, where the crossing point between the symmetries p- and d-wave is located.

concentration (n) for the same system as Fig. 1. In addition, Fig. 2b) shows the condensation energy (E_{cond}) versus n. All the parameters are in units of $|t|$, with $t = -1$ eV. Notice that the maximum of Δ_p is slightly shifted with respect to that of T_c. This is due to the chemical potential, which is slightly different between $T = T_c$ and $T = 0$. However, for the purpose of this work the fit was made at the maximum of T_c.

Table II shows three cases with different values of n_{op} around 0.5, with their respective ground state (E_g) and condensation energies (E_{cond}). It is important to mention that E_{cond} is defined as the energy difference between the normal state at ($T = T_c$) and the superconducting state at ($T = 0$). In other words, E_{cond} is the energy gain of the system when it goes into superconducting state. Notice that E_{cond} around $n_{op} = 0.5$ is small but positive.

The p-wave symmetry can compete with s*- and d-wave symmetries for the ground state, making it essential to compare their respective ground-state energies to determine the most stable superconducting symmetry, which was shown in the Fig. 7 of reference [14]. However, for $n_{op} = 0.5$, s*-wave superconducting states attain their maximum critical temperatures at larger values of t', therefore for this case, the competition for the ground state is between p-and d-wave symmetries.

Table III shows the critical temperatures and condensation energies of d- and p-wave superconducting states. It is important to mention that for d-wave symmetry, the values in Table III correspond to $\delta = \delta_3 = 0$. All the other Hamiltonian parameters are the same as in the p-wave case.

The values of $-t'/t$ and n_{op} that lead to the maximum critical temperature $T_{c-\max}$ for each superconducting symmetry (p- and d-wave) are shown in Fig. 3a). Notice that d-wave and p-wave superconducting states with $\delta_3 = 0.08$ eV achieve their maximum critical temperatures at similar values of their second-neighbor hoppings and electron densities. At $(-t^{'}/t, n_{op}) = (0.29, 0.5)$, the ground state energy for p-wave is $E_{pw-g-T_0} = -0.768070$ eV, which in comparison with d-wave case at the close point $(-t^{'}/t, n_{op}) =$

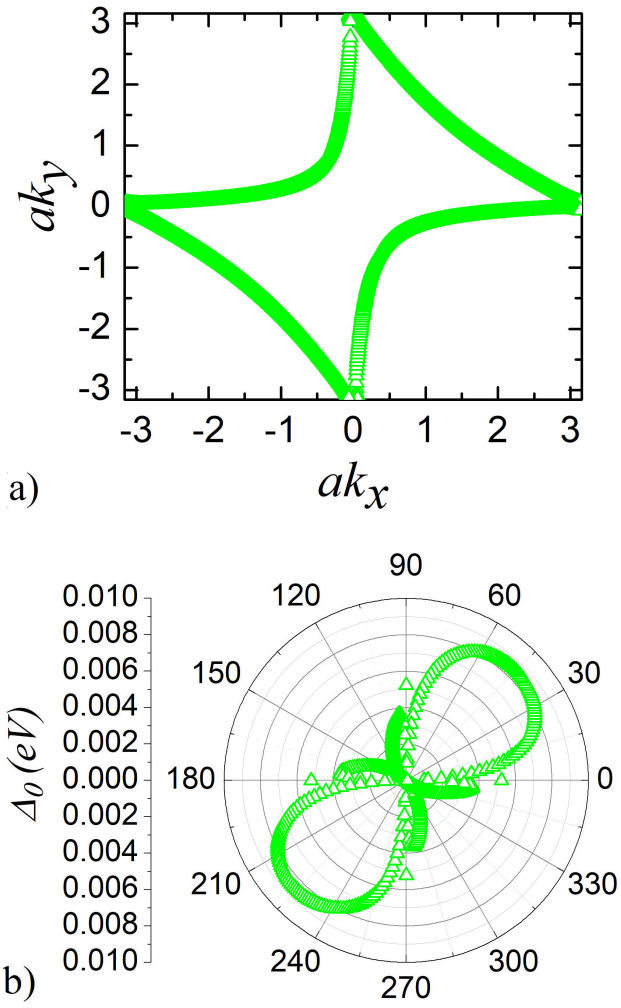

FIGURE 4. a) Fermi surface ($E_F = -1.354$ eV) for a superconducting system with $\Delta t = 0.5$ eV, $\Delta t_3 = 0.05$ eV, $\delta = 0.05$ eV, $\delta_3 = 0.08$ eV, $-t'/t = 0.29$, and $n_{op} = 0.5$. b) Single-particle excitation energy gap (Δ_0) for the same system as in Fig. 4a) and $\Delta_{p-max}/|t| = 0.00455$.

$(0.29, 0.49)$ is lower, since $E_{dw-g-T_0} = -0.73622$ eV, as indicated in Table III. Notice that d-wave has both $T_{c-\max}$ and E_{cond} higher. Moreover, calculating the d-wave case with $\delta = 0.05$ eV and $\delta_3 = 0.08$ eV, the corresponding $E_{dw-g-T_0} = -0.75064$ eV, which is higher than p-wave. Therefore, the system with the selected set of Hamiltonian parameters favors the p-wave symmetry, and it can be considered as the ground state in competition with d-wave case.

Figure 4a) shows the Fermi surface (FS) of a system chosen from Fig. 1, for which the p-wave T_c attains the highest value. Notice that the FS touches the frontier of the first Brillouin zone. Figure 4b) shows the corresponding single-particle excitation energy gap $[\Delta_0(\theta)]$ as a function of the angle $\theta = \tan^{-1}(k_y/k_x)$, where the p-wave-like symmetry is evident. $\Delta_0(\theta)$ is defined as the minimum value of $E(k_x, k_y)$, given by Eq. (12), along the θ direction. At the antinode, the energy necessary to break a Cooper pair is $\Delta_0/|t| \approx 2\Delta_p = 0.009111$ while $\Delta_0/|t| = 0.008503$. The superconducting

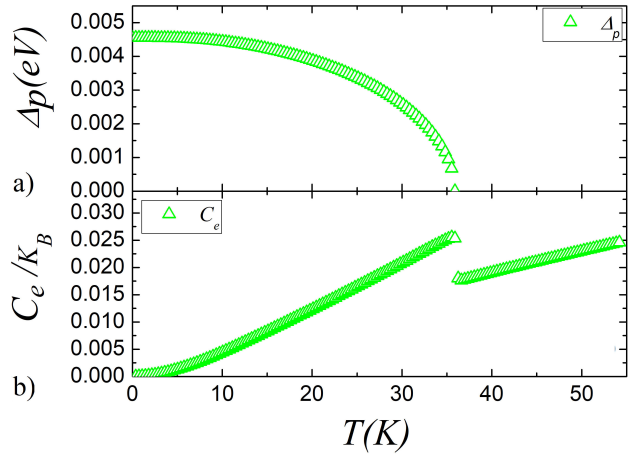

FIGURE 5. a) p-wave superconducting gap (Δ_p) versus temperature (T) for the same system as in Fig. 1 with $n_{op} = 0.5$. b) The corresponding p-wave electronic specific heat (C_e) versus temperature (T).

gap $\Delta_p = 0.00455$ eV agrees with the value 0.00472 eV experimentally found in tapes of $Sr_{1-x}K_xFe_2As_2$ [15].

To provide an additional comparison between theory and experimental data of $Sr_{0.5}K_{0.5}Fe_2As_2$, the electronic specific heat as a function of the temperature $C_e(T)$ and its corresponding jump (ΔC) at T_c, $\Delta C = [C_S(T_c) - C_N(T_c)]/C_N(T_c)$ were calculated [16]. The Eq. (19) gives the electronic specific heat (C_e) as a function of the temperature, where $\beta = 1/(k_B T)$, $f(E_k)$ is the Fermi-Dirac distribution, and E_k is the quasi-particles energy, given by Eq. (12). The results for $C_e(T)$ are shown in Fig. 5b). Notice that $\Delta C = 0.41$ and the corresponding $\Delta C/T_c = 94.7$ mJ/mol K^2, which is close to the value of 71.3 mJ/mol K^2 measured in $Sr_{1-x}K_xFe_2As_2$ superconductors [15].

$$C_e = \frac{2k_B\beta^2}{4\pi^2}\int\int_{1BZ} f(E_k)[1-f(E_k)] \cdot \left[(E_k)^2 + \beta E_k \frac{dE_k}{d\beta}\right]. \quad (19)$$

Since $C_e(T)$ depends on $E_k(T)$, it is necessary to calculate the temperature dependence of the superconducting gap amplitude $\Delta_p(T)$. Figure 5a) shows Δ_p versus T for $n_{op} = 0.5$ with all other model parameters kept the same as in Fig. 1. The curvature of Δ_p as a function of T determines the corresponding C_e shown in Fig. 5b). Moreover, it is expected that the curvature of this function will be different for each superconducting gap symmetry [17].

4. Conclusions

Our calculations show that doping $Sr_{1-x}K_xFe_2As_2$ near x=0.5 yields a maximum T_c of approximately 36 K for p-wave symmetry, in close agreement with the experimental value of 37 K. This quantitative agreement suggests that triplet pairing cannot be excluded in pnictides, particularly

under optimal doping. Furthermore, the calculated condensation energy is small but positive, consistent with experimental calorimetric data, and the specific heat jump (ΔC) at T_c matches well with the available measurements. Together, these results point toward a physically viable p-wave superconducting state. Comparison with other symmetries highlights the novelty of our findings. Previous works using the generalized Hubbard model have emphasized d-wave states, which can reach higher calculated T_c values under certain parameter choices [18]. However, when correlated hopping asymmetries are included, our results show that the p-wave state attains the lowest ground-state energy, thereby becoming the most stable configuration despite its smaller gap amplitude. The energy criterion determines the actual ground state, whereas higher T_c values alone do not guarantee stability. Our results therefore extend earlier studies by demonstrating that p-wave pairing can not only compete with but also exceed d-wave in stability under realistic conditions. The physical consequences of stabilizing a triplet p-wave state in pnictides are far-reaching. Unlike d-wave superconductors, where the spatial wavefunction is symmetric and spins form singlet pairs, p-wave superconductors host parallel-spin Cooper pairs with antisymmetric spatial components. This configuration can alter the magnetic response, allowing the superconductor to sustain higher external fields without pair breaking. If confirmed experimentally, such behavior in $Sr_{1-x}K_xFe_2As_2$ would distinguish it from cuprates and align it more closely with spin-triplet systems like Sr_2RuO_4, but at a significantly higher T_c. Additionally, our analysis suggests that other pnictides, such as $Ba_xK_{1-x}Fe_2As_2$ (with T_c up to 38 K) [19, 20], could exhibit similar behavior. Exploring p-wave stability across this family could provide a unifying framework for understanding unconventional pairing in Fe-based superconductors. Nonetheless, some limitations remain since our model considers a single band, while real materials involve multiband effects and orbital complexity. Future work should extend the generalized Hubbard framework to multiband models, enabling more direct comparison with ARPES and neutron scattering experiments. In summary, our results indicate that the generalized Hubbard model, when applied with suitable correlated hopping parameters, can describe p-wave superconductivity in $Sr_{1-x}K_xFe_2As_2$. The agreement of the calculated T_c value with the experimental one, consistent thermodynamic properties, and favorable ground-state energetics supports the possibility of triplet pairing in this compound, opening new perspectives for both theoretical and experimental investigations of high-T_c triplet superconductors.

Acknowledgments

The authors acknowledge the computer resources, technical expertise, and support provided by the Laboratorio Nacional de Supercómputo del Sureste de México, CONAHCYT network of National Laboratories. Computations were performed at Cuetlaxcoapan of LNS-BUAP (Project 202501024C) and at Miztli of DGTIC-UNAM (Project LANCAD-UNAM-DGTIC-180). L.A.P. acknowledges support from UNAM-PAPIIT IN102923.

1. Y. Kamihara, H. Hiramatsu, M. Hirano, R. Kawamura, H. Yanagi, T. Kamiya, and H. Hosono, Iron-Based Layered Superconductor: LaOFeP, *J. Am. Chem.* **128** (2006) 10012, https://doi.org/10.1021/ja063355c.
2. H.-H. Wen, G. Mu, L. Fang, H. Yang and X. Zhu, Superconductivity at 25 K in hole-doped $(La_{1-x}Sr_x)OFeAs$, *J. EPL*, **82** (2008) 17009, https://dx.doi.org/10.1209/0295-5075/82/17009.
3. M. Pan, Z. Huang, H. F. Ma, Y. J. Cui, X.S. Yang, Y. Zhao, The Doping Effect on the Lattices and Electronic Structure in Superconducting Fe-based Compounds $Sr_{1-x}K_xFe_2As_2$, *J. Supercond. Nov. Magn.* **23** (2010) 985, https://doi.org/10.1007/s10948-010-0693-0.
4. E.F. Talantsev, In-plane p-wave coherence length in iron-based superconductors, *Results Phys.*, **18** (2020) 103339, https://doi.org/10.1016/j.rinp.2020.103339.
5. A.P. Mackenzie and Y. Maeno, The superconductivity of Sr_2RuO_4 and the physics of spin-triplet pairing, *Rev. Mod. Phys*. **75** (2003) 657, https://doi.org/10.1103/RevModPhys.75.657
6. S. Ran *et al.*, Nearly ferromagnetic spin-triplet superconductivity, *Science* **365** (2019) 684, https://doi.org/10.1126/science.aav864
7. K. Sasmal *et al.*, Superconducting Fe-Based Compounds $(A_{1-x}Sr_x)Fe_2As_2$ with A = K and Cs with Transition Temperatures up to 37K, *Phys. Rev. Lett*. **101** (2008) 107007, https://doi.org/10.1103/PhysRevLett.101.107007
8. J. Bardeen, L.N. Cooper, and J.R. Schrieffer, Theory of Superconductivity, *Phys. Rev.*, **108** (1957) 1175, https://link.aps.org/doi/10.1103/PhysRev.108.1175.
9. L.A. Pérez, J.S. Millán, and C. Wang, Superconducting gap symmetry determined by the electron density, *Physica B: Condensed Matter*, **378-380** (2006) 437, https://doi.org/10.1016/j.physb.2006.01.151.
10. J.S. Millán, L.A. Pérez, and C. Wang, p-wave superconductivity in a two-dimensional generalized Hubbard model, *Phys. Lett. A*, **335** (2005) 505 https://doi.org/10.1016/j.physleta.2004.12.080.
11. C.P. Bean, Magnetization of Hard Superconductors, *Phys. Rev. Lett.* **8** (1962) 250, https://doi.org/10.1103/PhysRevLett.8.250
12. J. Millán, J.S Millán, L.A. Pérez and H.S. Ruiz, Critical Current Density in d-Wave Hubbard Superconductors, *Materials* **15** (2022) 8969, https://doi.org/10.3390/ma15248969.

13. R. Balian and N.R. Werthamer, Superconductivity with Pairs in a Relative p Wave, *Phys. Rev.*, **131** (1963) 1553, https://link.aps.org/doi/10.1103/PhysRev.131.1553.

14. B. Millán, I.J. Hernández, L.A. Pérez, and J.S. Millan, Optimal electronic doping in p-wave superconductors, *Rev. Mex. Fís.*, **67** (2021) 061601. https://doi.org/10.31349/RevMexFis.67.061601.

15. C. Dong, C. Yao, H. Huang, X. Zhang, D. Wang and Y. Ma, Calorimetric evidence for enhancement of homogeneity in high performance $Sr_{1-x}K_xFe_2As_2$ superconductors, *Scripta Materialia*, **138** (2017) 114, https://doi.org/10.48550/arXiv.1706.03303.

16. L.A. Pérez, J.S. Millán, B.C. Domínguez and C. Wang, Electronic specific heat of anisotropic superconductors and its doping dependence, *J. Magn. Magn. Mater.*, **310** (2007) e129, https://doi.org/10.1016/j.jmmm.2006.10.110.

17. J.S. Millán, L.A. Pérez and C. Wang, Electronic Specific Heat of s-,p-, and d-wave Superconducting States. *AIP Conf. Proc.*, **850** (2006) 563, https://doi.org/10.1063/1.2354835.

18. B. Millán, L.A. Pérez and J. S. Millán, Optimal doping for d-wave superconducting ground states within the generalized Hubbard model, *Rev. Mex Fís.*, **64** (2018) 233, https://doi.org/10.31349/RevMexFis.64.233

19. M. Rotter, M. Tegel, and D. Johrendt, Superconductivity at 38 K in the Iron Arsenide $Ba_{1-x}K_xFe_2As_2$, *Phys. Rev. Lett.* **101** (2008) 107006. https://doi.org/10.1103/PhysRevLett.101.107006

20. S. Avci1 *et al.*, Phase Diagram of $Ba_{1-x}K_xFe_2As_2$, *Phys. Rev. B* **85** (2012) 184507, https://doi.org/10.1103/PhysRevB.85.184507